ELSEVIER

Journal of Power Sources 90 (2000) 170–175

JOURNAL OF POWER SOURCES

www.elsevier.com/locate/jpowsour

The effect of annealing on the electrochemical properties of $Zr_{0.5}Ti_{0.5}Mn_{0.5}V_{0.3}Co_{0.2}Ni_{1.1}$ alloy electrodes

X.G. Yang [a,*], Q.A. Zhang [a], K.Y. Shu [a], Y.L. Du [a], Y.Q. Lei [a], Q.D. Wang [a], W.K. Zhang [b]

[a] *Department of Materials Science and Engineering, Zhejiang University, 310027 Zhejiang, People's Republic of China*
[b] *Department of Applied Chemistry, Zhejiang University of Technology, 310014 Zhejiang, People's Republic of China*

Received 11 August 1999; received in revised form 16 January 2000; accepted 19 February 2000

Abstract

The annealing treatment was found to result in the improvement in the cyclic stability but the degradation of discharge capacity, activation and high-rate dischargeability for $Zr_{0.5}Ti_{0.5}Mn_{0.5}V_{0.3}Co_{0.2}Ni_{1.1}$ alloy electrode. A lower discharge potential in the annealed alloy electrode was found owing to a more homogeneous alloy, which is consistent with the pressure–composition isotherms (P–C–T) measurement. We found that the annealed alloy also had lower and flatter pressure plateaus, and larger pressure hysteresis. At high discharge rates, the hydrogen diffusion in the bulk of the alloy was the rate-determining step. The diffusion coefficients for hydrogen in the annealed and as-cast alloys were calculated to be 1.4×10^{-12} cm^2 s^{-1} and 4.3×10^{-12} cm^2 s^{-1}, respectively. The lowering of high-rate discharge capacity can be ascribed to the reason that the hydrogen diffusion coefficient is lower due to homogeneous microstructure in the annealed alloy.

Keywords: Hydrogen storage alloy; Annealing treatment; Electrochemical property; Homogeneity; Hydrogen diffusion coefficient; P–C–T

1. Introduction

Systematic substitution with metal elements has been applied to the Zr-based Laves phase hydrogen storage alloys to improve the electrochemical properties, because the ZrM_2 hydrides (M = V, Cr and Mn) are thermodynamically too stable to release hydrogen easily at the ambient condition. Alloying with other transition metals has been proven effective for expediting the hydrogen desorption without too much degrading hydrogen storage capacity, improving high-rate discharge/charge ability, cyclic lifetime and activation, etc. Generally, chemical substitution leads to changes in phase structure and phase abundance as well as the hydrogen storage performance [1]. Hout et al. [2] investigated the effect of substituting in (Zr, A)$V_{0.5}Ni_{1.1}Mn_{0.2}Fe_{0.2}$ (A = Ti, Nb or Hf) alloys on the relationship between phase composition and electrochemical capacity and found that the alloys with C15 as its main phase displayed a large reduction in discharge capacity when the discharge current was high, but the alloys composed of C14 main phase showed much better high-rate dischargeability. However, the contribution of different types of Laves phases (C14 or C15) to the high-rate capacity was found to be contrary for the Ti-free and Ti-substituted Zr-based hydride electrodes [3]. It is the fact that substitution of Ti for Zr will effectively increase the specific discharge capacity, because Ti possesses only half atomic quantity of that of Zr. Alloying with Ti would also decline thermodynamics stability of its hydride. It was reported that Ti substitution for Zr by 20% (atomic) in an AB_2 type alloy increases the equilibrium pressure of plateau by 5 times, 30% induces 10 times [4]. High concentration of Ti reduces the strict requirement for pure raw materials and makes the alloy preparation more practical. We experimentally found that $Zr_{0.5}Ti_{0.5}Mn_{0.5}V_{0.3}Co_{0.2}Ni_{1.1}$ alloy exhibited a discharge capacity more than 350 mA h g^{-1}. In our series compositional optimization [5], we also found that the promising molar ratio of V/(V + Mn) for favorable electrochemical performances ranges from 2/9 to 4/9. Mn alloying can flatten and increase the pressure plateau without capacity degradation, and make the alloy

* Corresponding author. University of Hawaii, Holmes Hall 246, 2540 Dole Street, Honolulu, HI 96822, USA.
E-mail address: xgyang@usa.net. (X.G. Yang).

0378-7753/00/$ - see front matter
PII: S0378-7753(00)00406-7

mechanically brittle, easily pulverized during activation processes. V alloying enables enlarging the hydrogen storage capacity, and more effectively in the presence of Ti substitution. However, the electrochemical stability of the as-cast alloy $Zr_{0.5}Ti_{0.5}Mn_{0.5}V_{0.3}Co_{0.2}Ni_{1.1}$ is not satisfied even if alloyed with the stabilizing element Co, because partially of the severe oxidation of Ti and the heterogamous microstructures. Lee et al. [6] reported that the annealed $ZrV_{0.7}Mn_{0.5}Ni_{1.2}$ exhibited a higher discharge efficiency than comparable as-cast alloy, owing the improvement to Ni dissolving into matrix from the second phase. Another investigation on $ZrNi_{1.2}Mn_{0.6}V_{0.2}M_W$ (M = Cr, Co, Mo or Al, $w = 0.05$ or 0.1) system hydride electrodes by Knosp et al. [7] showed that the annealing treatment (1323 K for 7 days) could reduce the phase abundance of Zr_7Ni_{10} or Zr_9Ni_{11} from 10–25 wt.% to 5%, and increase the discharge capacity from about 350 to 370 mA h g^{-1}. In the present paper, we apply the annealing treatment to the Ti-substituted alloy, and attempt to investigate its resultant effect on the electrochemical properties, crystalline, thermodynamics and microstructure.

2. Experimental

$Zr_{0.5}Ti_{0.5}Mn_{0.5}V_{0.3}Co_{0.2}Ni_{1.1}$ alloy was prepared in an induction furnace under argon atmosphere. The purity of the constituent metals was all above 99.9%. The annealing treatment was performed at 1273 K for 8 h on the as-cast alloy under vacuum (at about 10^{-2} Pa). Both the as-cast and annealed alloys were crushed mechanically in air.

Powder X-ray diffraction data were obtained from the sieved powders (−43 μm) of the inactivated alloys by using *Rigaku C-max*-III *B* Diffractometer with a Cu K_α radiation and a nickel-diffracted beam filter. The microstructure of the alloys was studied by using Leica DML optical microscope. The metallographic samples held in special clamps were milled first on sand papers, and then polished in a polishing machine with Al_2O_3 powder at a rotation rate of 1350 rpm for about 25 min. The pressure–composition isotherm (P–C–T) measurement was performed in an automatic P–C–T test apparatus after the alloy powders (about 1 g) have been activated by at least five hydrogenation/dehydrogenation cycles.

The hydride electrodes were prepared by cold pressing the mixtures of different alloy powders (−42 μm) with powdered electrolytic copper (42 μm) in the weight ratio of 1:2 to form porous 10-mm-diameter pellets in copper holders. Electrochemical charge–discharge tests were carried out in a standard open trielectrode electrolysis cell, in which the counter-electrode was nickel oxyhydroxide, the reference electrode was Hg/HgO/6 M KOH, and the electrolyte was 6 M KOH solution. The discharge capacities of hydride electrodes were determined by galvanostatic method. The Tafel plots are measured cathodically scanning the fully charged hydride electrodes at a rate of 100 mV/s. The equilibrium potentials of the as-cast and annealed alloy electrodes in full charge state are measured to be −0.947 V and −0.937 V vs. Hg/HgO at 298 K, respectively.

3. Results and discussion

The activation process and the cyclic lives of the as-cast and the annealed alloys are shown in Fig. 1A and B. Both alloys are easily activated within two to three cycles. Our previous study revealed that a few tens of initial charge/discharge cycles are needed to activate the Ti-free alloy electrodes [3]. The good activation property for the present alloys substituted with titanium make them possible for practical applications. It is also one of most important reasons for that the Ovonic patented electrode alloys consist of concentrated Ti component. We found that after annealing at 1273 K for 8 h, the maximum discharge capacity decreases from 353 mA h g^{-1} for the as-cast alloy to 321 mA h g^{-1}. However, the cycling stability is improved by the annealing treatment as shown in Fig. 1B.

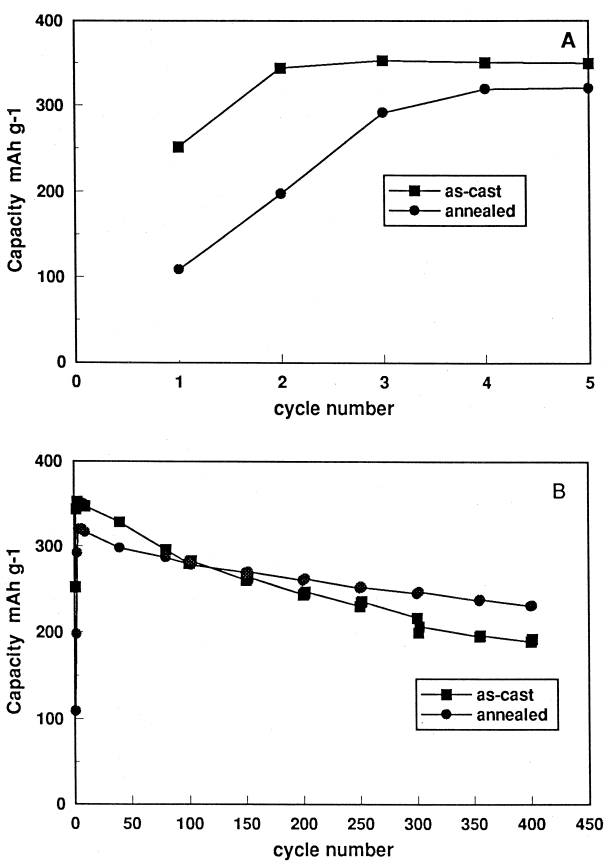

Fig. 1. The electrochemical properties of $Zr_{0.5}Ti_{0.5}Mn_{0.5}V_{0.3}Co_{0.2}Ni_{1.1}$ alloy, (A) activation and (B) the cyclic lifetime. Discharge current 50 mA g^{-1}.

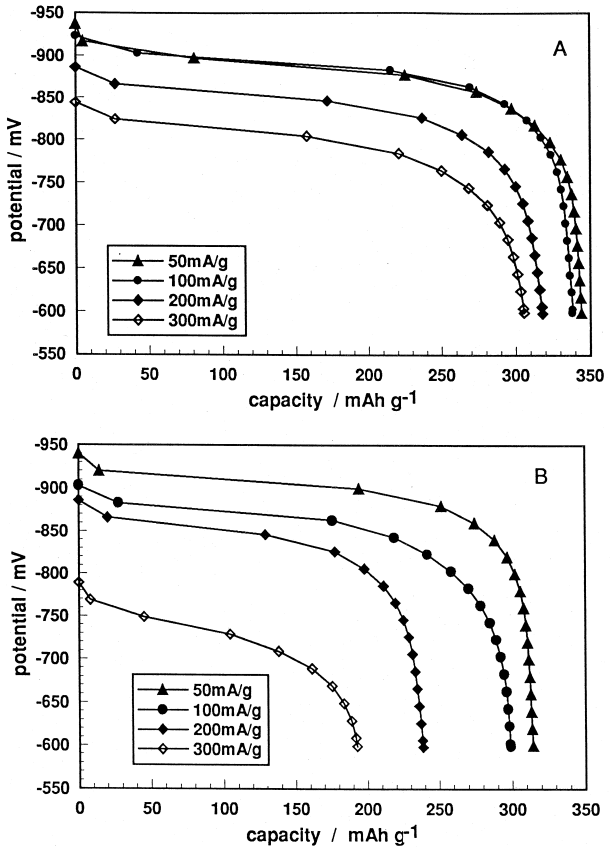

Fig. 2. The discharge potential curves at different currents 100–300 mA g^{-1} for as-cast (A) and annealed (B) alloys $Zr_{0.5}Ti_{0.5}Mn_{0.5}V_{0.3}Co_{0.2}Ni_{1.1}$ at 298 K.

The as-cast electrode retains only 55% of its maximum capacity, whereas the annealed one returns charge by as high as 72% after 400 cycles.

The discharge potential profiles of the as-cast and annealed electrodes at different current densities 50–300 mA g^{-1} are depicted in Fig. 2A and B. For the as-cast alloy, the potential–capacity curves at 50 and 100 mA g^{-1} are almost the same. While for the annealed electrode, the discharge potential plateau at 100 mA g^{-1} is obviously positive by about +350 mV compared to that at 50 mA g^{-1}. As the discharge current is up to 300 mA g^{-1}, the trend in the reduction of capacity and larger polarization are much more clear. In the same figures, the starting potentials of the discharge curves, which are measured when the discharge currents are applied to, are not the theoretical values at 0 mA g^{-1} because of our low-rate data acquisition system. But the more positive potentials could also show the large burden of electrochemical reaction of the annealed electrode. Usually, the equilibrium potential of a fully charged hydride electrode is taken the theoretical value of −0.92 V (vs. Hg/HgO) for either single electrode or battery simulations. However, we experimentally estimated the equilibrium potentials varying with different hydride electrodes. Electrodes with high concentration of Zr, V or Cr exhibit more negative potentials, i.e., −0.965 V for a Zr–Cr–Ni electrode. This deviation in equilibrium potentials from the theoretical value is ascribed to the various surface chemical states of electrodes.

The discharge potential of hydride electrode consists of three main contributions, namely, from electrochemical reaction, hydrogen diffusion within the bulk of the alloy, and solution resistance and contact resistance [8]. When the discharge current is high or the hydrogen concentration is relatively low, the hydrogen diffusion is regarded as the rate-determining step. The discharge process will be stopped due to the great diffusion overpotential. The annealing treatment decreases hydrogen diffusion kinetics and reduces the discharge efficiency, therefore, decreases the discharge capacity. The high-rate discharge ability degrades in the annealed AB_2 type electrode as shown in Fig. 3. The initial hydrogen storage capacities are nearly the same if both lines are extrapolated to intercept the ordinate at $i = 0$ mA g^{-1}. It implies that the annealing treatment changes the hydrogen diffusion kinetics rather than degrades the hydrogen storage capacity.

Assuming that the hydride particles for the as-cast and annealed alloys are in spherical form with an average radius of a, which is about 2 μm estimated by SEM observation. According to Fick's second law, the diffusion equation for hydrogen in a spherical particle can be written as

$$\frac{\partial(rc)}{\partial t} = D\frac{\partial^2(rc)}{\partial r^2} \quad (1)$$

where c is the concentration of hydrogen in the alloys, t is time of diffusion, D is the average diffusion coefficient and r is the distance from the center of the sphere.

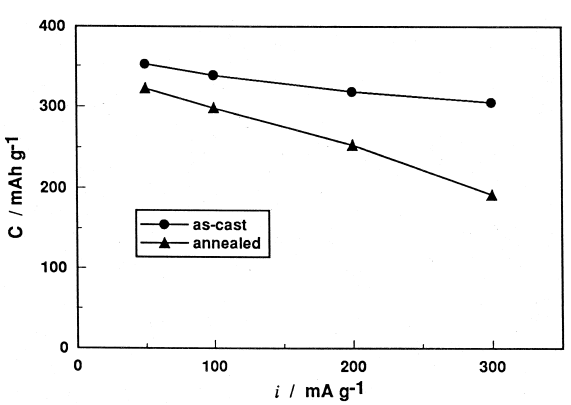

Fig. 3. The dischargeability of the as-cast and annealed alloy electrodes at 298 K.

Under the constant current condition, the constant flux of the hydrogen at the surface was assumed to homogeneous. The value of D/a^2 may be determined for a long diffusion period (or a large transitions time τ) according to the equation by Zheng et al. [9]

$$\frac{D}{a^2} = \frac{1}{15\left(\frac{Q_0}{i} - \tau\right)} \quad (2)$$

where Q_0 is the initial specific hydrogen capacity (C/g), i is the discharge current density (A/g), and τ is the transient time (s), when the hydrogen surface concentration becomes zero. The ratio Q_0/i corresponds to the discharge time necessary to discharge completely the electrode under hypothetical conditions when the discharge proceeds without interference of diffusion.

When the discharge current is large, the rate-determining step may transfer into the hydrogen diffusion process. The nominal hydrogen diffusion coefficients in the as-cast and annealed electrode alloys could be estimated to be 4.3×10^{-12} cm^2 s^{-1} and 1.4×10^{-12} cm^2 s^{-1} at the discharge current of 300 mA g^{-1}, respectively. The value of D for the as-cast alloy is larger by three times than that for the annealed alloy.

Fig. 4A and B depicts the XRD patterns of the as-cast and annealed alloys. It is found that both the as-cast and annealed alloys have the main phase of hcp C14 Laves phase, altogether with some fcc C15 Laves phase and a trace of Zr_7Ni_{11}. However, in the annealed alloy, the abundance of main phase C14 is found to decrease slightly,

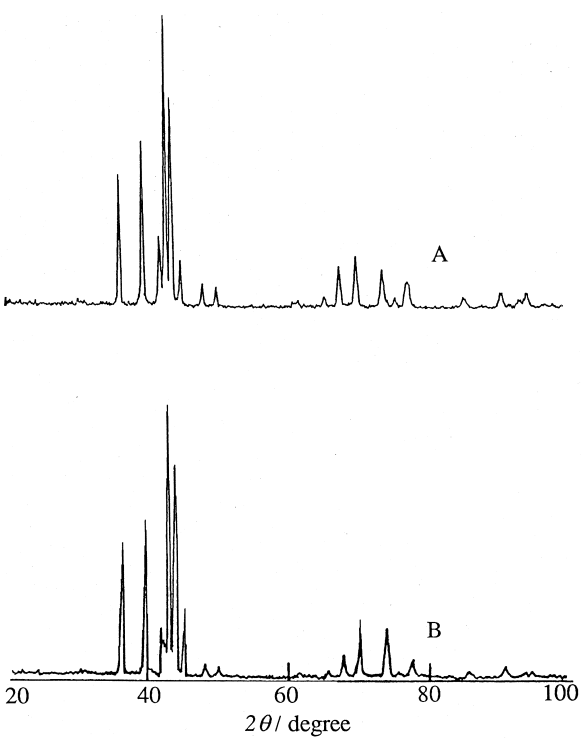

Fig. 4. The XRD patterns of the (A) as-cast and (B) annealed alloys.

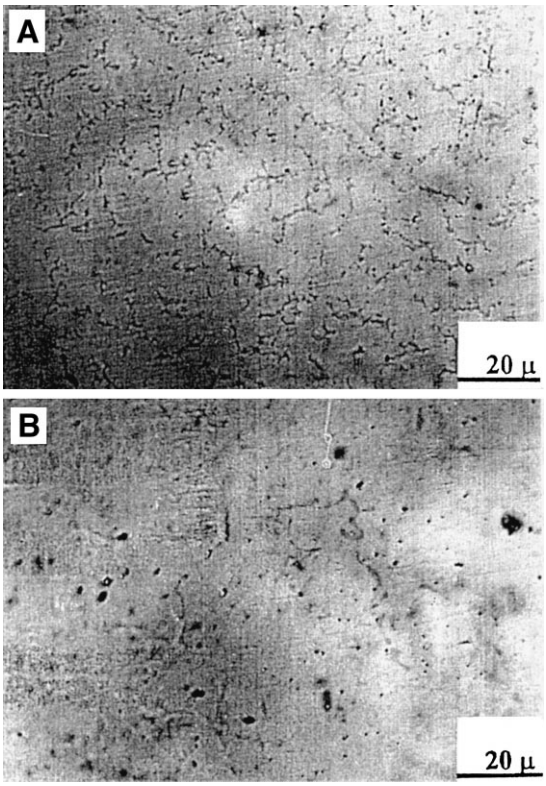

Fig. 5. The optic morphologies of the as-cast (A) and annealed (B) alloys.

the crystalline characteristics is getting more perfect and the stress reduces markedly because the XRD peaks narrow obviously, which is consistent with other investigation on Zr–Cr–Ni system alloys [10]. The Laves phase (C15 or C14) is doubtlessly considered as hydrogen storage reservoir, but different Laves phases have varied electrochemical behaviors in Ti-containing or Ti-free hydride electrodes [3].The second phase Zr_7Ni_{10} serves as the electrochemical catalyst, the aggregation of which incurred from annealing treatment reduces the specific surface area.

The microstructural features of both the as-cast and annealed alloys were studied by optical microscopy as shown in Fig. 5. The observed samples were finely polished without etching. From Fig. 5A, the average grain size of the as-cast alloy was estimated to be about 10 μm from the clear boundaries, where the C15 phase was believed to precipitate. Some more dark spots existing along the boundaries could be the Zr_7Ni_{10} phase. However, the boundaries of the annealed alloy become vague, and the dark spots aggregate more spherically and clearly stick out along the boundaries throughout the observed scope. The homogeneity is brought about after annealing, therefore, the better anticorrosion and longer cyclic lifetime of the annealed alloy can be explained. Meanwhile, the annealing induces a negative effect on the discharge kinetics due to the reduction in proton diffusion coefficient. The multi-phase structure and defects in the bulk of hydride alloys could affect their electrode performance

markedly, the microstructural homogeneity induced by annealing provides less diffusion channels for hydrogen and increases the diffusion energy barrier [11].

We further examined the pressure–concentration isotherms in the gas-phase condition as shown in Fig. 6. The maximum hydrogen-desorbing capacities of both alloys are almost the same, which is consistent with our hypothesis deduced from Fig. 3. However, the as-cast alloy exhibits very small hysteresis and slightly higher pressure plateau, while the plateau of the annealed alloy shows more plain, as we can anticipate from its equilibrium electrode potentials. Therefore, we believe that the decrease in the dischargeability of the annealed alloy might result partly from the low flat pressure plateau and large hysteresis instead of the hydrogen storage capacity. In another word, the phase and structure disorder will benefit electrochemical discharge property of AB_2 multiphase alloys, especially the kinetics.

The equilibrium potentials of the as-cast and annealed alloy electrodes in full charge state are measured to be -0.947 and -0.937 V vs. Hg/HgO at 298 K, respectively. According to the Nernst equation, a more negative potential refers to a higher hydrogen equilibrium pressure of the hydride. The Tafel plots of the as-cast and annealed alloy electrodes $Zr_{0.5}Ti_{0.5}Mn_{0.5}V_{0.3}Co_{0.2}Ni_{1.1}$ during charging are shown in Fig. 7. The cathodic overvoltage is a little higher for the annealed electrode than that for the as-cast. It implies that the annealing treatment reduces the charging efficiency as well as the discharge efficiency. The similar Tafel slopes indicate that the mechanism for hydrogen evolution is the same for both electrodes. The total exchange current density i_0 is found to be ca. 204 mA g^{-1} for the as-cast and 157 mA g^{-1} for the annealed by extrapolating the Tafel line to the intercept at $\eta = 0$. Thus the i_0 consists of two parts: $i_{0,\upsilon}$ for the Volmer reaction ($H_2O + e^- \rightarrow H(a) + OH^-$) and for the Tafel reaction ($H(a) + H(a) \rightarrow H_2$).Therefore, the larger i_0 for the as-cast

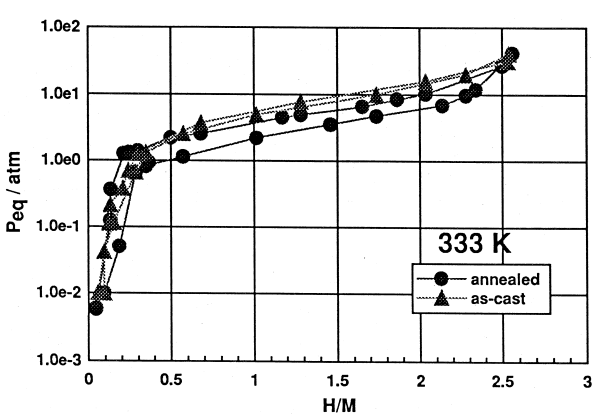

Fig. 6. The pressure–concentration isotherms ($P-C-T$) at 333 K of the as-cast and annealed alloys $Zr_{0.5}Ti_{0.5}Mn_{0.5}V_{0.3}Co_{0.2}Ni_{1.1}$.

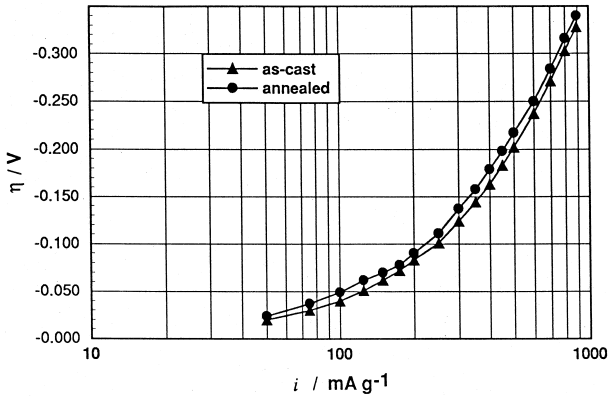

Fig. 7. Cathodic polarization curves of the as-cast and the annealed alloy electrodes.

electrode indicates that the Volmer reaction is accelerated, showing better catalytic characteristics.

4. Conclusion

The annealing treatment (1273 K for 8 h) improves the cyclic stability but shows a negative effect on the discharge capacity, activation and the high-rate dischargeability of $Zr_{0.5}Ti_{0.5}Mn_{0.5}V_{0.3}Co_{0.2}Ni_{1.1}$ alloy electrode. A larger polarization and poorer kinetics were found in the annealed alloy because of the phase composition and structural homogeneity. During discharge process at a large current density, the hydrogen diffusion is regarded as the rate-determining step. The hydrogen diffusion coefficient in the as-cast alloy electrode was calculated to be 4.3×10^{-12} cm^2 s^{-1}, which is larger by three times than 1.4×10^{-12} cm^2 s^{-1} in the annealed alloy. The small coefficient D is believed to be a result out of the homogenization incurred by annealing treatment.

Acknowledgements

This work is supported by National Advanced Materials Committee of China and National Natural Science Foundation of China (59601006).

References

[1] J.M. Joubert, D.L. Sun, M. Latroche, A. Percheron-Guegan, J. Alloys Compd. 253 (1997) 564.
[2] J. Hout, E. Akiba, T. Osura, Y. Ishido, J. Alloys Compd. 218 (1995) 101.
[3] X.G. Yang, W.K. Zhang, Y.Q. Lei, Q.D. Wang, J. Electrochem. Soc. 146 (4) (1999) 1245.
[4] D.G. Ivey, D.O. Northwood, J. Mater. Sci. 18 (1983) 321–347.
[5] W.K. Zhang, Y.Q. Lei, X.G. Yang, Q.D. Wang, Trans. Nonferrous Met. Soc. China 7 (3) (1997) 59.
[6] S.M. Lee, D.M. Kim et al., J. Electrochem. Soc. 145 (1998) 1953.

[7] B. Knosp, C. Jordy, Ph. Blanchard, T. Berlureau, J. Electrochem. Soc. 145 (5) (1998) 1478.
[8] Q.M. Yang, M. Ciureanu, D.H. Ryan, J.O. Strom-Olsen, J. Electrochem. Soc. 141 (1994) 2108.
[9] G. Zheng, B.N. Popov, R.E. White, J. Electrochem. Soc. 142 (1995) 2693.
[10] J.M. Joubert, M. Latroche, A. Percheron-Guegan, J. Alloys Compd. 24 (1996) 219.
[11] D. Richter, R. Hempelmann, R.C. Bowman Jr., in: L. Schlapbach (Ed.), Hydrogen in Intermetallic Compounds: II. Surface and Dynamics Properties, Applications, Springer, Berlin, 1992, p. 97.